MAGNETOHYDRODYNAMICS Vol. 37 (2001), No. 1-2, pp. 71–79

ON THE RESULTS OF THE RIGA DYNAMO EXPERIMENTS

A. Gailitis[1], *O. Lielausis*[1], *E. Platacis*[1], *G. Gerbeth*[2], *F. Stefani*[2]

[1] *Institute of Physics, University of Latvia, Salaspils-1, LV-2169, Latvia*
[2] *Forschungszentrum Rossendorf, P.O. Box 510119, D-01314 Dresden, Germany*

On 11 November 1999, magnetic field self-excitation was observed for the first time in a hydromagnetic experiment at the Riga dynamo facility. In a second experiment in July 2000, the dynamo behaviour in the kinematic as well as in the saturation regime was studied. We report on the results of both experiments and try to understand the saturation mechanism.

Introduction. The primary goal of the Riga dynamo experiment is to study the basic physical phenomenon of magnetic field self-excitation in electrically conducting fluids rather than to simulate the magnetic field generation process of a particular cosmic body. Experimental dynamos can be divided into "guided" and "free" flow dynamos. On this scale, the Riga dynamo can be located in the middle. As will be shown, the sodium flow is "guided" and regular enough to allow a rather precise prediction of the kinematic dynamo behaviour. On the other hand, due to the fact that the azimuthal velocity component is kept only by inertia, the flow is free enough to allow the Lorentz forces not only to increase the overall losses but also to change the velocity structure.

1. The experimental design. The experiment represents the technical realization of what could be called an "elementary cell" of any hydromagnetic dynamo: a helical flow. The basic idea goes back to Ponomarenko [1] who considered magnetic field self-excitation in an electrically conducting solid cylinder screwing through a medium at rest with the same conductivity. Gailitis and Freibergs found in 1976 [2] that the field can grow if the magnetic Reynolds number $\mathrm{Rm} = \mu_0 \sigma v_{max} R$ exceeds a value of 17.7 (μ_0 is the permeability of the vacuum, σ is the electrical conductivity, v_{max} is the maximal velocity, R is the radius of the cylinder).

An important modification of the original Ponomarenko model which turns the convective instability of this model into an absolute instability is the addition of a co-axial back-flow [3]. Additionally it is useful to provide the system with a third co-axial cylinder containing sodium at rest. This part makes electric currents close in a larger volume by which the Ohmic losses are decreased. Such a type of dynamo was optimized with respect the main geometric relations thus fixing the length and the diameters of the three cylinders [4].

Five years were devoted to the installation of a water test facility and of the final sodium facility. The test runs with water turned out crucial for the success of the later sodium experiments as it was necessary to optimize the velocity profiles in order to reach self-excitation within the given motor power limitations. This iterative process, including theoretical and numerical profile optimization [5], pump design and velocity measurements [6] was finished in 1998.

Until the first experiment could start, it took again more than a year to finish all necessary preparations. The central module of the experimental facility

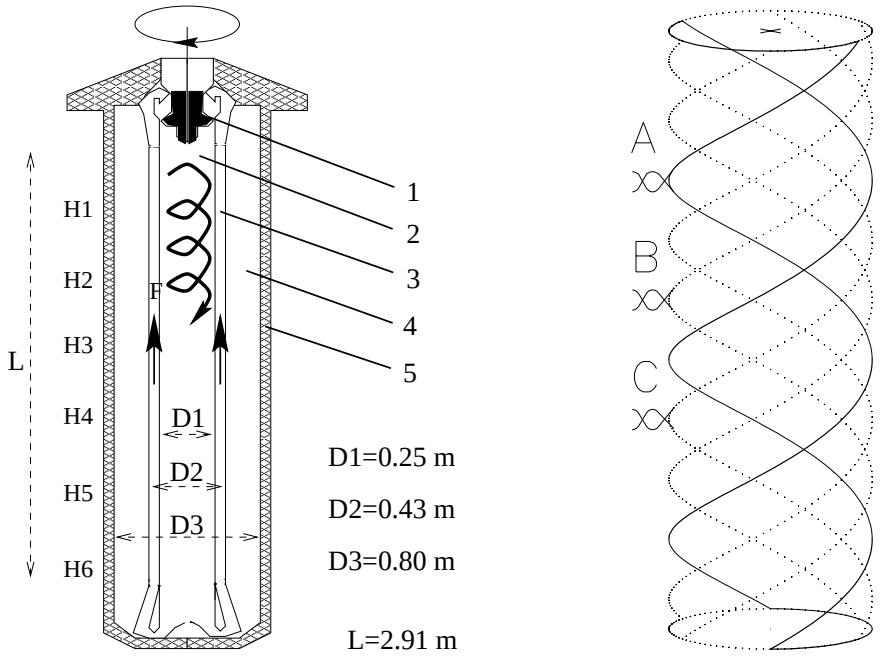

Fig. 1. The central module of the Riga dynamo facility: *1* – propeller, *2* – helical flow region, *3* – back-flow region, *4* – sodium at rest, *5* – thermal insulation F – position of the flux-gate sensor and the measuring induction coil, H1...H6 – positions of Hall sensors.

Fig. 2. Three phase coil wound around the dynamo module. The geometry of the seed field resulting from this coil is similar to the geometry of the eigenmode of the dynamo. The same coil was used as a measuring device giving an integral value of the generated magnetic field.

is shown in Fig. 1. Fig. 2 shows the three phase coil which was wound around the module and which served as a seed field coil in the sub-critical regime and as an additional measuring device in the critical regime.

2. The first experiment in November 1999. The first experiment in November 1999 has been described in [7], so that we can restrict ourselves here to a sketch of the main results. The bulk of measurements in November was devoted to the amplification of a seed field which was externally applied by the special three phase coil (Fig. 2). When the current in this coil was switched off, the field was decaying with a decay time depending on the rotation rate.

Fig. 3 shows such a magnetic field decay as it was observed for a rotation rate of 1980 rpm at the six Hall sensors (H1...H6 in Fig. 1). This observed field was already an eigenmode of the dynamo which can be concluded from those well-identifiable features as, e.g., phase and amplitude relation between the signals at the different sensors H1...H6, frequency, and growth rate which was still slightly negative.

Whereas for all rotation rates until appr. 2100 rpm with the seed field switched on the only observation was a sinusoidal signal with the frequency of the seed field, at 2150 rpm the situation changed essentially. Fig. 4 shows the measured signal and its decomposition into the amplified seed field and another signal with a remarkably different frequency and, this time, with a slightly positive growth

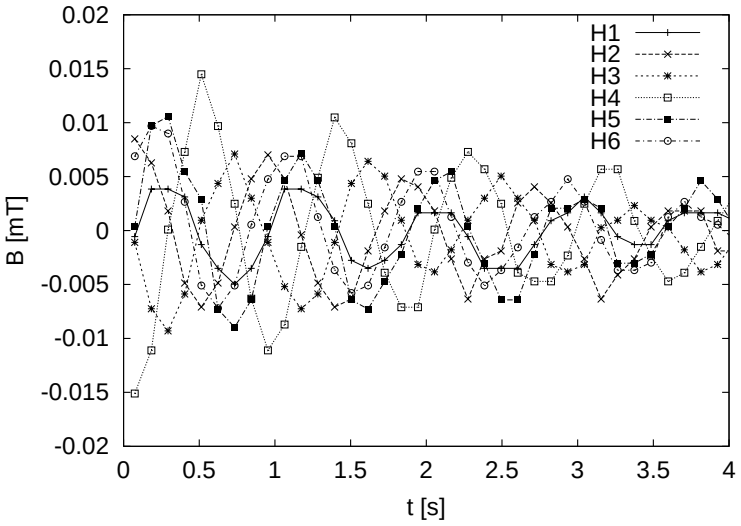

Fig. 3. Radial magnetic field component measured at the six Hall sensors H1...H6 outside the dynamo module after switching off the coil current at a rotation rate of 1980 rpm and a temperature of 210°C. All signals show the same exponential decay with a growth rate of $p = -0.3s^{-1}$ and the same frequency of 1.1 Hz.

rate. By means of careful data analysis this mode was clearly identified as an exponentially growing eigenmode of the dynamo.

3. The second experiment in July 2000 – a typical run. In July 2000, it was possible to work at considerably lower temperatures (down to 153°C) and therefore at higher Rm. In total, we have carried out four runs with a duration between 8 and 15 minutes each. Three runs were conducted temporarily with a seed field and one run was conducted without any seed field. In [8] we have documented the run without any seed field, thus we will present here one run where the seed field has been temporarily switched on.

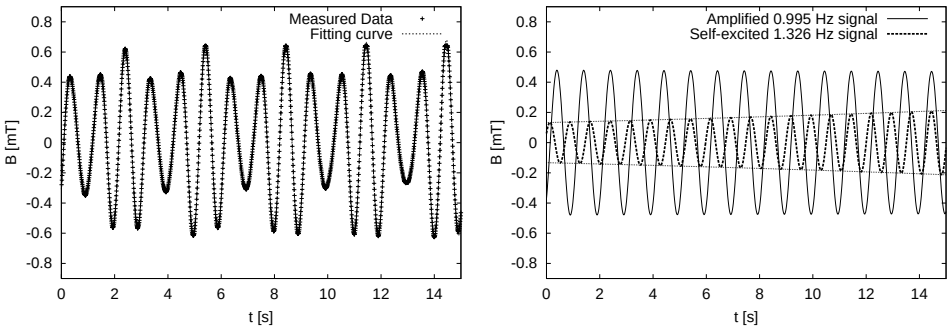

Fig. 4. Magnetic field signal measured at 2150 rpm at the flux gate sensor F and fitting curve (left). Decomposition of the fitting curve into two curves with different frequencies (right). The growth rate of the 1.326 Hz signal was $p = +0.03s^{-1}$.

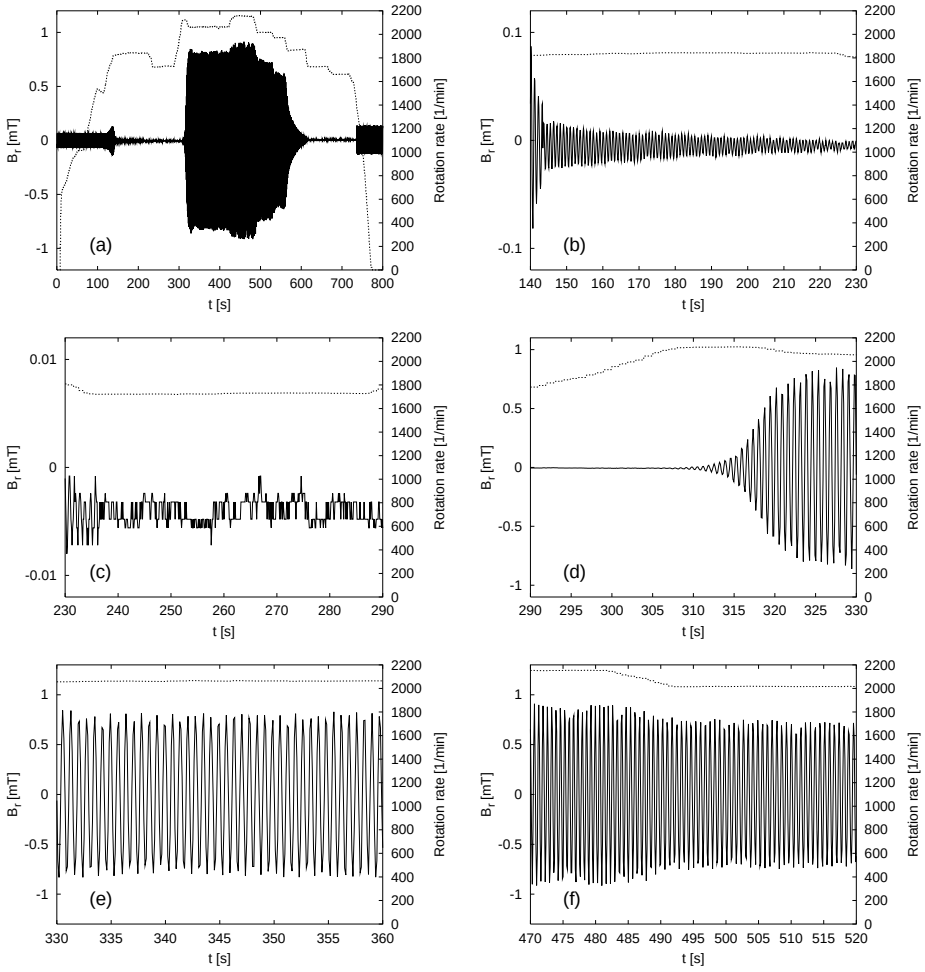

Fig. 5. A typical run in July 2000. Full picture (a), extremely slow decay (b), nothing than noise (c), self-excitation and transition to the saturation regime (d), saturation regime with constant rotation rate (e), saturation regime with changing rotation rate (f).

Fig. 5 illustrates this run showing the rotation rate of the propeller and the signal at one selected Hall sensor (H4). Fig. $5a$ documents this run as a whole, the remaining Figs $5b - 5f$ show details of the course of events (note that the interval lengths in Figs $5b - 5f$ are not identical). The current in the seed field coils was switched on at the beginning (from 0–143 sec) and at the end (from 736–815 sec). The large "bulk" in the middle of Fig. $5a$ represents the period with self-excitation, where the magnetic field amplitude obviously depends on the rotation rate.

Let us describe this run a bit more in detail. At the very beginning of Fig. $5b$ the seed field was switched off as we wanted to study the free decay of the field which we expected to be already slow. The rotation rate of 1840 rpm at this moment was already very close to the critical rotation rate. This is evident from the extremely slow decay of the magnetic field with a decay rate of $p = -0.0184 s^{-1}$ (i.e, it takes 38 seconds for the field to decrease by a factor 2). This time interval of more than a minute is very interesting as it contains practically the signal of a pure kinematic dynamo (note that $p = -0.0184 s^{-1}$ is not very different from zero

if compared, say, with $p = +0.36s^{-1}$ as in Fig. 5*d*).

Having seen this "unending" signal at 1840 rpm, we decided to lower the rotation rate until 1720 rpm and to keep it there for a minute (Fig. 5*c*) in order to let the magnetic field disappear before the very self-excitation was to be studied.

After this had happened, we drove the rotation rate quickly up to 2050 rpm and kept it constant there (Fig. 5*d*). In this figure we see how an oscillating magnetic field emerges "from nothing" and how it saturates later at a amplitude of about 1 mT. Note that this 1 mT has been measured at H4, i.e. outside the dynamo facility. Much larger field amplitudes have been found at the inner sensors as described in [8]. Fig. 5*e* illustrates the magnetic field behaviour within the saturated regime with the rotation rate kept constant. Fig. 6f shows how the saturation level decreases with decreasing rotation rate.

4. Collection of main results. From all experimental runs conducted in November and July, we have assembled in Fig. 6 the measured growth rates (*a*) and frequencies (*b*) in dependence on the rotation rate and the temperature. We have taken into account only those time intervals where the rotation rate was kept constant. Most of the data were recorded during field decays after the seed field had been switched off. A few points with positive growth rate correspond to the kinematic phase of self-excitation when the saturation regime had not been reached yet. Only in the frequency plot in Fig. 6*b*, there are also some points in the saturation regime which will concern us below.

As for the growth rates and the frequencies in the kinematic regime, the correspondence of the measured data and the predicted curves is quite convincing. Notable is a slight shift of the measured growth rate data of about 10 per cent towards higher rotation rates and an overall shift of the frequency data of about 5 percent towards lower rotation rates. In both cases the slopes of the curves as well the temperature dependence are in good agreement with the predictions.

As far as the saturation regime is concerned, we show in Fig. 7 for one experimental run the mechanical motor power consumption as a function of the rotation rate Ω. We have carefully taken into account only data from those time intervals where the rotation rate was kept constant not in order to bias the results by acceleration effects. As expected from hydraulic arguments, the data in the field-free regime are best fitted with an Ω^3 curve. The deviation of the four rightmost points in the saturation regime from this Ω^3 curve shows, however, that there is evidently an increase of the power consumption which must be explained in terms of the back-reaction of the magnetic field. Note that we have used a passport efficiency of 87 per cent for the electric motors in order to get the points in Fig. 7. A more detailed investigation of this efficiency in dependence on the rotation rate which is carried out presently might lead to slight corrections of Fig. 7.

In order to estimate this additional power due to the induced currents one can compute the Ohmic losses $P_{\rm Ohm} = \int j^2/\sigma \, {\rm d}V$. Using for this purpose, as a first rough estimate, the magnetic field structure as it results from the kinematic code and fixing its strength to the measured field strength we get Ohmic losses of approximately 10 kW. Fig. 7 shows that this is in good correspondence with the observed power consumption increase.

This increase of the power consumption can as well be explained by computing the pressure increase due to the axial component of the Lorentz force. Indeed, this calculation leads to nearly the same increase of motor power consumption.

However, it is not possible to absorb the axisymmetric part of the the azimuthal component the Lorentz force into pressure. Hence, this force should have a breaking effect on the azimuthal component of the velocity. An observable feature pointing on such a velocity change can be inferred from Fig. 8. In this plot

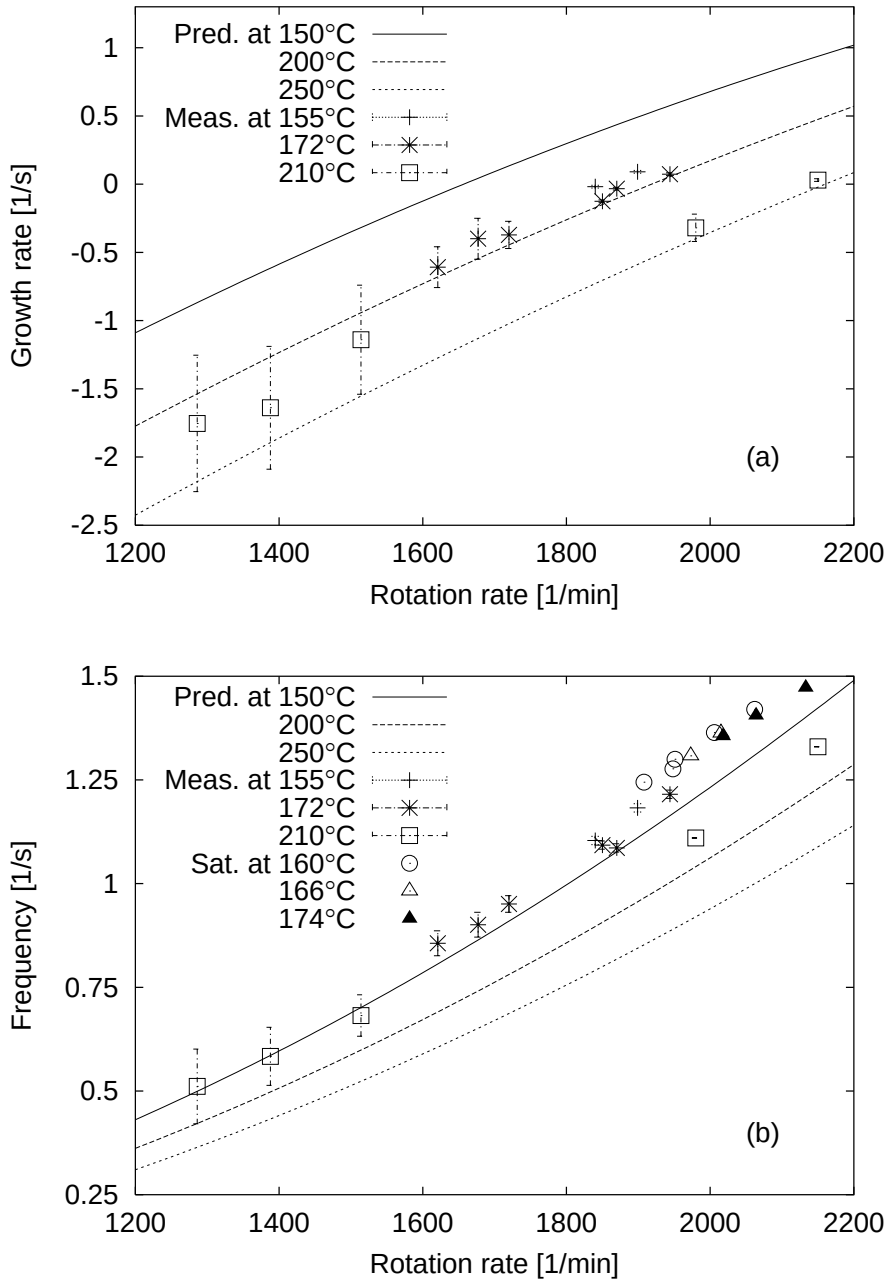

Fig. 6. Growth rates (a) and frequencies (b) measured in November 1999 and July 2000 experiments for different rotation rates and temperatures, and corresponding numerical predictions. The shown temperatures are to be understood as $\pm$ 3°C. The larger error bars at low rotation rates are due to the fact that for a quickly decaying signal the frequency and the decay rate are much harder to determine than for a slow decaying or an increasing signal. In (b) the frequencies in the saturation regime are also given, whereas the corresponding growth rates are zero.

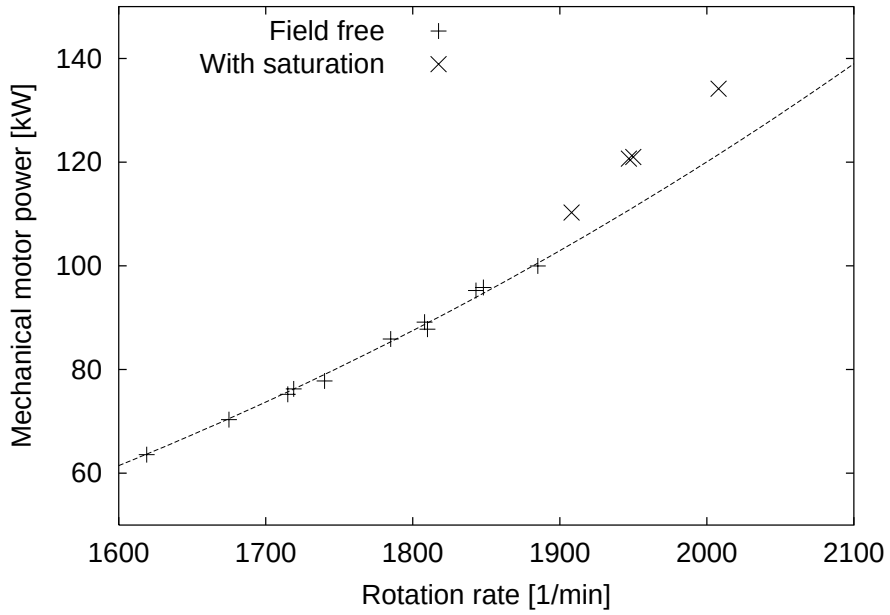

Fig. 7. Motor power below and in the saturation regime. The broken line represents a Ω^3 behaviour as it comes out of a fit of the points in the field free regime and which is also well-known from hydraulics.

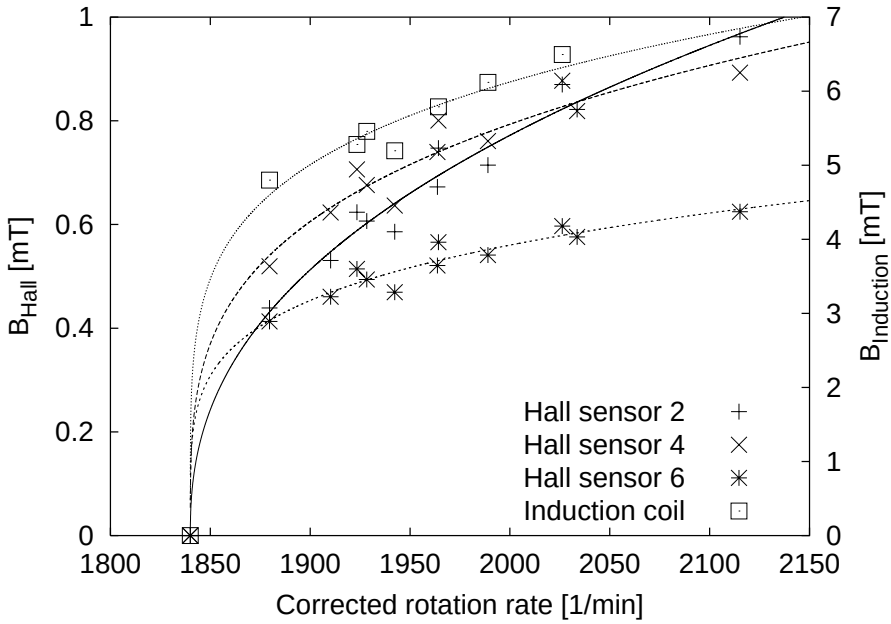

Fig. 8. Measured magnetic field levels in the saturation regime. The corrected rotation rate Ω_c is related to the measured rotation rate Ω via $\Omega_c(T) = \sigma(T)/\sigma(157^\circ\mathrm{C})\,\Omega$. The point at 1840 rpm is taken as a marginal reference point as the growth rate at this point was practically zero.

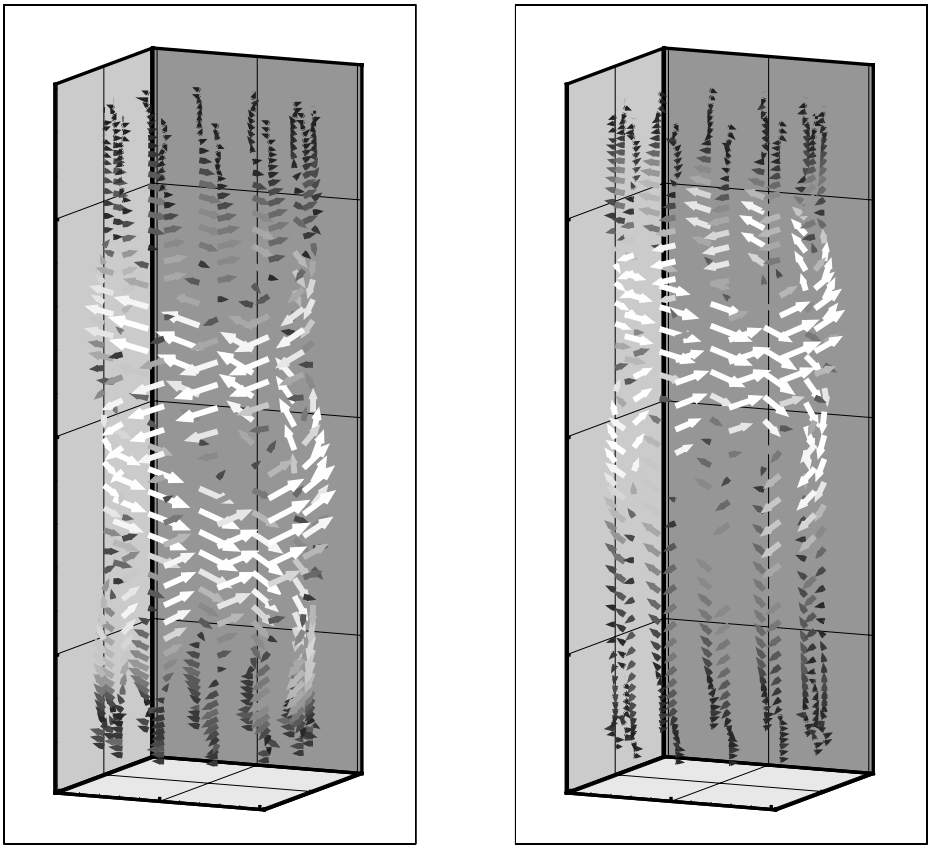

Fig. 9. Predicted magnetic field structure for the kinematic regime (left) and for the strongly damped azimuthal velocity component (right). The plots illustrate the magnetic field structure at a radius very close to the innermost wall. Note that z-axis is compressed by a factor 5. The brighter the arrows, the larger is the length of the vectors. The shift of the field maximum towards the top (the propeller region) is clearly visible.

the dependence of the magnetic field amplitude measured at the Hall sensors H2, H4, and H6 and at the induction coil F on the corrected rotation rate Ω_c is given. Clearly visible is a increasing shift of the field amplitude maximum towards the propeller region with increasing rotation rate.

Another interesting fact is that the frequencies in the saturation regime continue to grow (Fig. 6*b*) whereas at the same time the growth rates are (by definition) zero (Fig. 6*a*). This is a second serious hint that there must be a significant deformation of the velocity field apart from an overall pressure increase due to the Lorentz forces.

Now we can try to reproduce these two features of the back-reaction which go beyond the power increase by simply assuming a certain decay of the azimuthal velocity component along the z-axis. To take a concrete value, let us suppose that the velocity at two third of the total length from above is reduced to 0.7 of the velocity which was assumed in the computations for the kinematic case. Fig. 9 shows the resulting shift of the maximum towards the propeller region. Qualitatively, this corresponds very well with the observed behaviour. What is more, for the deformed velocity the frequency stays basically the same whereas the growth rate decreases significantly.

Therefore, such downward decay of the azimuthal velocity is a good candidate to explain the magnetic field saturation in the experiment. Of course, this has to be supported by further numerical analysis and, hopefully, by direct velocity measurements inside the dynamo.

5. Conclusions. After years of preparation, including the well-aimed determination of the overall flow geometry, the design of the whole facility with careful considerations of all requirements of sodium technique, and experimental fine-tuning of the velocity profiles based on extensive computer simulations, the Riga dynamo has turned out as a neatly working hydromagnetic facility which is well-predictable in the kinematic regime and which shows already a non-trivial behaviour in the saturation regime. The whole installation is ready for a number of additional experiments where the back-reaction and the MHD turbulence can be studied.

Acknowledgments. We thank the Latvian Science Council for support under grant 96.0276, the Latvian Government and International Science Foundation for support under joint grant LJD100, the International Science Foundation for support under grant LFD000 and Deutsche Forschungsgemeinschaft for support under INK 18/B1-1. We are grateful to W. Häfele for his interest and support, and to the whole experimental team for preparing and running the experiment.

REFERENCES

1. Yu. B. Ponomarenko. On the theory of hydromagnetic dynamo. *J. Appl. Mech. Tech. Phys.* vol. 14 (1973), pp. 775–779.
2. A. Gailitis and J. Freibergs. To the theory of a helical MHD–dynamo. *Magnetohydrodynamics*, vol. 12 (1976), pp. 127–129.
3. A. Gailitis and J. Freibergs. Nature of instability in a helical MHD dynamo. *Magnetohydrodynamics*, vol. 16 (1980), pp. 116–121.
4. A. Gailitis. Project of a liquid sodium MHD dynamo experiment. *Magnetohydrodynamics*, vol. 32 (1996), pp. 58-62.
5. F. Stefani, G. Gerbeth, and A. Gailitis. Velocity profile optimization for the Riga dynamo experiment. in: *Transfer Phenomena in Magnetohydrodynamic and Electroconducting Flows*, edited by A. Alemany, Ph. Marty, J. P. Thibault, Kluwer Academic Publishers, Dordrecht (1999), pp. 31–44.
6. M. Christen, H. Hänel, and G. Will. Entwicklung der Pumpe für den hydrodynamischen Kreislauf des Rigaer "Zylinderexperimentes". in: *Beiträge zu Fluidenergiemaschienen 4*, edited by W. H. Faragallah, G. Grabow, Faragallah-Verlag und Bildarchiv, Sulzbach/Ts. (1998), pp. 111–119.
7. A. Gailitis, O. Lielausis, S. Dement'ev, E. Platacis, A. Cifersons, G. Gerbeth, Th. Gundrum, F. Stefani, M. Christen, H. Hänel, and G. Will Detection of a flow induced magnetic field eigenmode in the Riga dynamo facility. *Phys. Rev. Lett.*, vol. 84 (2000), pp. 4365–4368.
8. A. Gailitis, O. Lielausis, E. Platacis, S. Dement'ev, A. Cifersons, G. Gerbeth, Th. Gundrum, F. Stefani, M. Christen, and G. Will Magnetic field saturation in the Riga dynamo experiment. *Phys. Rev. Lett.*, vol. 86 (2000), pp. 3024–3027.

Received 01.02.2001